

PDF hosted at the Radboud Repository of the Radboud University Nijmegen

This full text is a publisher's version.

For additional information about this publication click this link.

<http://hdl.handle.net/2066/16321>

Please be advised that this information was generated on 2014-11-13 and may be subject to change.

Hartree-Fock-Slater-LCAO calculations on the Cu(II) bis(dithiocarbamate) complex; magnetic coupling parameters and optical spectrum

P. J. M. Geurts, P. C. P. Bouten, and A. van der Avoird

Institute of Theoretical Chemistry, University of Nijmegen, Toernooiveld, Nijmegen, The Netherlands
(Received 10 July 1979; accepted 16 April 1980)

The electronic structure of the copper (II) bis(dithiocarbamate) complex has been calculated by the nonempirical Hartree-Fock-Slater-LCAO method and, from the resulting molecular orbitals, the g tensor and the copper and sulfur hyperfine tensors have been obtained. The bonding between the Cu atom and the four ligand S atoms is mainly covalent and the unpaired electron is delocalized over these atoms. All the magnetic parameters are in fair agreement with the experimental EPR results and also the electronic excitation energies agree rather well with the optical spectrum.

I. INTRODUCTION

Transition metal complexes with dithiocarbamate ligands have been the subject of extensive studies in our department¹ and elsewhere.² Especially about the complex bis(N, N'-diethyl-dithiocarbamate) copper(II), $\text{Cu}(\text{et}_2\text{dtc})_2$, rather complete information is available; from EPR we know the g tensor and the (an)isotropic metal and sulfur hyperfine tensors,³⁻⁵ the polarized optical spectrum has been measured,⁶ and the redox potentials have been obtained.⁷ Extended Hückel (EH) molecular orbital calculations have been performed^{8,9} by adjusting two of the EH parameters such that the calculated principal values of the g tensor agree with experiment. This gave quite good agreement also between the calculated anisotropic hyperfine tensors and the experimental values so that we can assume that the (valence) molecular orbital (MO) picture thus obtained is realistic. Still, other properties, e.g., the electronic excitation energies, are badly represented by the EH method and, moreover, it is rather uncertain whether the parameter choice obtained from this "calibration" procedure⁸ has any general significance. Therefore, there is a need for *ab initio* quantum theoretical methods applicable to transition metal complexes, which are necessarily more complicated than the simple semiempirical EH method, but which may provide more generally reliable information about the electronic structure of such complexes even if only few data are available from experiment. Such a method is the nonempirical Hartree-Fock-Slater linear combination of atomic orbitals (HFS-LCAO) method developed by Ros and Baerends^{10,11} which has already been tested on a series of small molecules and some transition metal complexes.¹² So far, no attention has been given to the calculation of magnetic properties by this method. The $\text{Cu}(\text{dtc})_2$ complex seems a very suitable case to test this method for ligands of a different type and also to look at the accuracy of some procedures proposed for calculating magnetic coupling parameters from the HFS molecular orbitals.

II. METHODS

A. Molecular orbital method

The Hartree-Fock-Slater LCAO method has been described in detail elsewhere.^{10,11} Its most characteris-

tic features are the replacement of the Hartree-Fock one-electron exchange operator by a local ($X\alpha$) potential depending on the (spin) density¹³ and the representation of this (spin) density by a linear combination of exponential (Slater-type) functions centered on the nuclei. (We have included density fit functions of s , p , d , f , and g type; no spherical averaging of the density or the potential around the nuclei takes place, in contrast with the HFS-scattered wave method¹⁴ which uses a muffin-tin potential.) A similar density fitting procedure in terms of s -type Gaussian functions has been proposed by Sambe and Felton.¹⁵ The matrix elements of the Coulomb and exchange operators derived from this (fitted) density are calculated numerically.¹⁰ The exchange parameter α was kept at 0.7 as in all previous calculations with this method.^{11,12}

We have used both the spin-polarized, unrestricted (UHFS) and the restricted (RHFS) versions of the method.¹² The atomic orbital basis set used in most calculations comprised the $3d$, $4s$, $4p$ orbitals for Cu, $3s$, $3p$ for S, $2s$, $2p$ for C and N, $1s$ for H, each represented by two Slater-type orbitals (STO's, double zeta basis), the core orbitals (represented by near Hartree-Fock functions¹⁶) were frozen, i.e., a constant contribution from the core electrons has been included in the Coulomb and exchange potentials, while all valence orbitals have been orthogonalized to the core by adding linear combinations of STO's, one for each core orbital. In one calculation these single zeta core orbitals on Cu were explicitly included in the secular problem in order to observe the effect of core (spin) polarization. All orbital exponents have been taken from the tables by Clementi and Roetti.¹⁶ Computer timings for this HFS-LCAO method applied to transition metal complexes compare favorably with the Hartree-Fock-LCAO method.¹⁷

B. Expressions for magnetic coupling parameters

1. g tensor

The system we are dealing with has a spin-doublet ground state with no orbital degeneracy (Cu $3d^9$ if the complex were completely ionic). We can write the following approximate second-order perturbation formula for the g tensor.^{18,19} (Δg_{ij} is the deviation from the free-electron result g_e ; $i, j = x, y, z$)

$$\Delta g_{ij} = g_e \sum_{m,\sigma} \sum_{n,\sigma'} \sum_A \sum_B \frac{\langle \chi_m^A | \xi^A(r_A) L_i^A | \chi_n^A \rangle \langle \chi_n^B | L_j^B | \chi_m^B \rangle}{\epsilon_m - \epsilon_n} \quad (1)$$

The first summation refers to the occupied spin-orbitals, the second to the virtual spin-orbitals ($\sigma' = \sigma$); A and B run over all atoms. Actually, the second-order contribution to Δg is only gauge invariant together with a first-order term; expression (1) corresponds to a particular gauge in which this first-order term is negligible.^{18,19} Furthermore, one must make the following assumptions in deriving it.

(i) Spin-orbit coupling can be described by an (effective) one-electron operator, i.e., the two-electron coupling terms^{20,21} can be taken into account by an effective one-electron potential. This approximation seems consistent with the HFS (independent particle) formalism used for the calculation of the molecular (spin) orbitals. The functions $\chi_{m,n}^{A,B}$ occurring in formula (1) are the restrictions of the molecular orbitals $\Psi_{m,n}$ to the atoms A, B; they include the MO coefficients. We have taken these orbitals, both the occupied, Ψ_m , and the virtual ones, Ψ_n , and the corresponding orbital energies, ϵ_m and ϵ_n , from a ground state HFS calculation. In this respect, it is important to remember that the excited wave functions are not necessarily the best descriptions of the physical excited states of the system; the only condition required by perturbation theory is that they form (or, in practice, approach) a complete set together with the ground state functions. Expression (1) with this choice of $\Psi_{m,n}$ and $\epsilon_{m,n}$ corresponds with uncoupled Hartree-Fock(-Slater) perturbation theory.²²

(ii) The effective one-electron potential occurring in the spin-orbit coupling terms is a scalar potential which can be additively constructed from contributions spherical around the nuclei; the corresponding electric field felt by the electrons is

$$\mathbf{E} = \frac{2m^2c^2}{e\hbar^2} \sum_A \xi^A(r_A) \mathbf{r}_A \quad (2)$$

The operators L_i^A , L_j^B are components of the angular momentum around the nuclei A, B.

(iii) Only one-center integrals are retained. It has been shown by Moores and McWeeny²¹ that the approximations (i)-(iii) produce results for the spin-orbit splitting in NO and CH and the g tensor in NO₂ and CN which are in good agreement with the results of complete *ab initio* calculations including all two-electron spin-orbit coupling terms and many-center integrals. If the em-

pirical values for the atomic spin-orbit parameters, λ^A , are introduced for the radial matrix elements over $\xi^A(r_A)$, the results are in excellent agreement also²¹ with the molecular experimental data. This explains the success of the usual semiempirical description of spin-orbit coupling effects by the operator $\sum_A \lambda^A \mathbf{L}^A \cdot \mathbf{S}$.^{18,23} Extending formula (1) with many-center terms seems easy, but it requires the *ab initio* calculation of matrix elements for which we need explicitly the effective scalar and vector potential accounting for all two-electron coupling terms, while the results would probably be less accurate.²¹ So we have chosen to use formula (1) with the empirical atomic spin-orbit parameters from Table I. The only problem then is that we have a double zeta representation for each atomic orbital (AO) which leads to three different (two diagonal and one off-diagonal) radial matrix elements over $\xi^A(r^A)$ while only one empirical parameter λ^A is available per AO. We have solved this problem by assuming that $\xi^A(r^A)$ depends on r^A as $(r^A)^{-3} Z_{\text{eff}}^{20}$, calculating the three matrix elements over $(r^A)^{-3}$ and distributing λ^A proportionally over the corresponding $\xi^A(r^A)$ matrix elements. The error which we possibly introduce by this procedure must remain very small, since by far the largest contribution to λ^A arises from the single diagonal element over the most compact basis orbital and, moreover, the coefficients of the two exponential functions are not very different in the atom and in the molecule.

2. Hyperfine coupling tensor

The first, isotropic, hyperfine coupling contribution is the Fermi-contact term, which is directly proportional to the spin density at the nucleus, B.

$$a^B = \frac{8\pi}{3} \frac{\mu_0}{4\pi} g_e g_B \mu_b \mu_n \times \left(\sum_{m,(\sigma=\alpha)} |\Psi_m(B)|^2 - \sum_{m',(\sigma=B)} |\Psi_{m'}(B)|^2 \right), \quad (3)$$

where μ_b is the Bohr magneton, μ_n is the nuclear magneton, g_B is the gyromagnetic ratio of nucleus B, and μ_0 is the vacuum permeability. The summations both refer to the occupied spin orbitals. Next we have a first-order (anisotropic) electron-spin-nuclear-spin dipole-dipole term plus two second-order terms due to the additional coupling with the orbital angular momentum. If we make the same assumptions as in deriving the g tensor, we obtain the following expression (derived for the spin-restricted case in Refs. 24 and 25):

$$A_{ij}^B = \frac{\mu_0}{4\pi} g_e g_B \mu_b \mu_n \left[\left(\sum_{\substack{m,(\sigma=\alpha) \\ \text{occupied} \\ \text{spin} \\ \text{orbitals}}} \langle \chi_m^B | T_{ij}^B | \chi_m^B \rangle - \sum_{\substack{m',(\sigma=B) \\ \text{occupied} \\ \text{spin} \\ \text{orbitals}}} \langle \chi_{m'}^B | T_{ij}^B | \chi_{m'}^B \rangle \right) + \sum_{\substack{m,\sigma \\ \text{occupied} \\ \text{spin} \\ \text{orbitals}}} \sum_{\substack{n,\sigma' \\ \text{virtual} \\ \text{spin} \\ \text{orbitals} \\ (\sigma'=\sigma)}} \sum_A \left(\frac{2 \langle \chi_m^A | \xi^A(r^A) L_i^A | \chi_n^A \rangle \langle \chi_n^B | (r^B)^{-3} L_j^B | \chi_m^B \rangle}{\epsilon_m - \epsilon_n} + \sum_{k,l} i \epsilon_{kij} \frac{\langle \chi_m^A | \xi^A(r^A) L_k^A | \chi_n^A \rangle \langle \chi_n^B | T_{lj}^B | \chi_m^B \rangle}{\epsilon_m - \epsilon_n} \right) \right] \quad (4)$$

TABLE I. Spin-orbit coupling parameters λ .^a

Atom	Orbital	λ (cm ⁻¹)
Cu	3d	828
S	3p	382
C	2p	28
N	2p	76

^aFrom Refs. 8 and 24.

where T_{ij}^B is the dipole-dipole coupling tensor of an electron with nucleus B and ϵ_{kH} is the antisymmetric Levi-Cevita symbol.²⁶ The second-order terms in A_{ij}^B contain an isotropic (pseudo-contact) contribution which must be added to the Fermi-contact term (3).

Finally we must remark that, of course, the many-electron ground state wave function (Slater determinant) constructed with the molecular orbitals from a spin-unrestricted HFS calculation does not exactly correspond with a doublet spin eigenstate. The results show that the differences between orbitals for spin α and orbitals for spin β in our unrestricted calculations are quite small, however, and, therefore, we have not tried to correct the results for this defect. [This could be done by spin projection of the total wave function after the self-consistent-field (SCF) calculation²⁷ which is a cumbersome and still not very satisfactory procedure.] In our formulas for the magnetic coupling parameters we have assumed that the two components of a Kramers doublet can be represented by the wave functions resulting from two (formally) different UHFS calculations, one with an extra "unpaired" spin α and one with an extra spin β . Moreover, we have only considered those excitations in the second-order terms of Eqs. (1) and (4), which yield nonzero contributions if the α and β orbitals are exactly equal^{24,25} (i. e., the excitations of the "unpaired" electron to higher MO's and the excitations from lower MO's to the unpaired hole). In parallel with the spin-unrestricted calculations, we have also performed restricted HFS calculations.

C. Electronic excitation energies

In the HFS method the electronic excitation energies can be calculated as the difference between the relevant

orbital energies in a transition state calculation,¹³ where the transition state for each excitation is obtained by transferring half an electron (without changing spin). If the relaxation effects accompanying this electron transfer are small, one can also estimate the excitation energies from ground state orbital energy differences.

III. CALCULATIONS AND RESULTS

The EPR results have been obtained from studies of $\text{Cu}(\text{et}_2\text{dte})_2$ doped into single crystals of the diamagnetic $\text{Ni}(\text{II})(\text{et}_2\text{dte})_2$ complex.³⁻⁵ Since these results have indicated^{3,4} that the structure of the guest molecules $\text{Cu}(\text{et}_2\text{dte})_2$ is close to the $\text{Ni}(\text{et}_2\text{dte})_2$ structure, we have based our calculations on the structure of the latter compound.²⁸ The molecular symmetry of this compound is C_i but it deviates only slightly from D_{2h} symmetry and we have assumed this higher symmetry in our HFS-LCAO calculations, using the atomic coordinates shown in Fig. 1. Extended Hückel calculations which have been done previously^{8,9} in C_i symmetry and which we have now repeated in D_{2h} symmetry (see Fig. 2 and Tables II and III) yield practically identical results. Moreover, we have replaced the terminating ethyl groups by hydrogen atoms. Experiments with different alkyl-substituted ligands²⁹ and extended Hückel calculations²⁴ have shown that this replacement has no significant effect on the optical and magnetic properties studied in this paper.

The unrestricted HFS calculation with frozen cores on Cu, S, C, and N and the AO basis described above yields the MO level scheme in Fig. 2. Relaxing the core orbitals on Cu makes no visible difference in this (valence level) scheme (and in most other properties, except for the Fermi-contact term, see below). A restricted HFS calculation yields about the average result of the α and β levels from the unrestricted calculation (see Fig. 2). The ground state orbital occupancy can be read from this figure, with the "unpaired" electron occupying the $5b_{1g}$ orbital. This occupancy agrees with the EH calculations. The Cu-S bonding is mainly covalent, with rather small changes on the atoms and considerable positive overlap populations (see Table II). The unpaired electron is distributed rather evenly over the Cu $3d_{xy}$ orbital and the $3p_x$ and $3p_y$ orbitals of the four S atoms.

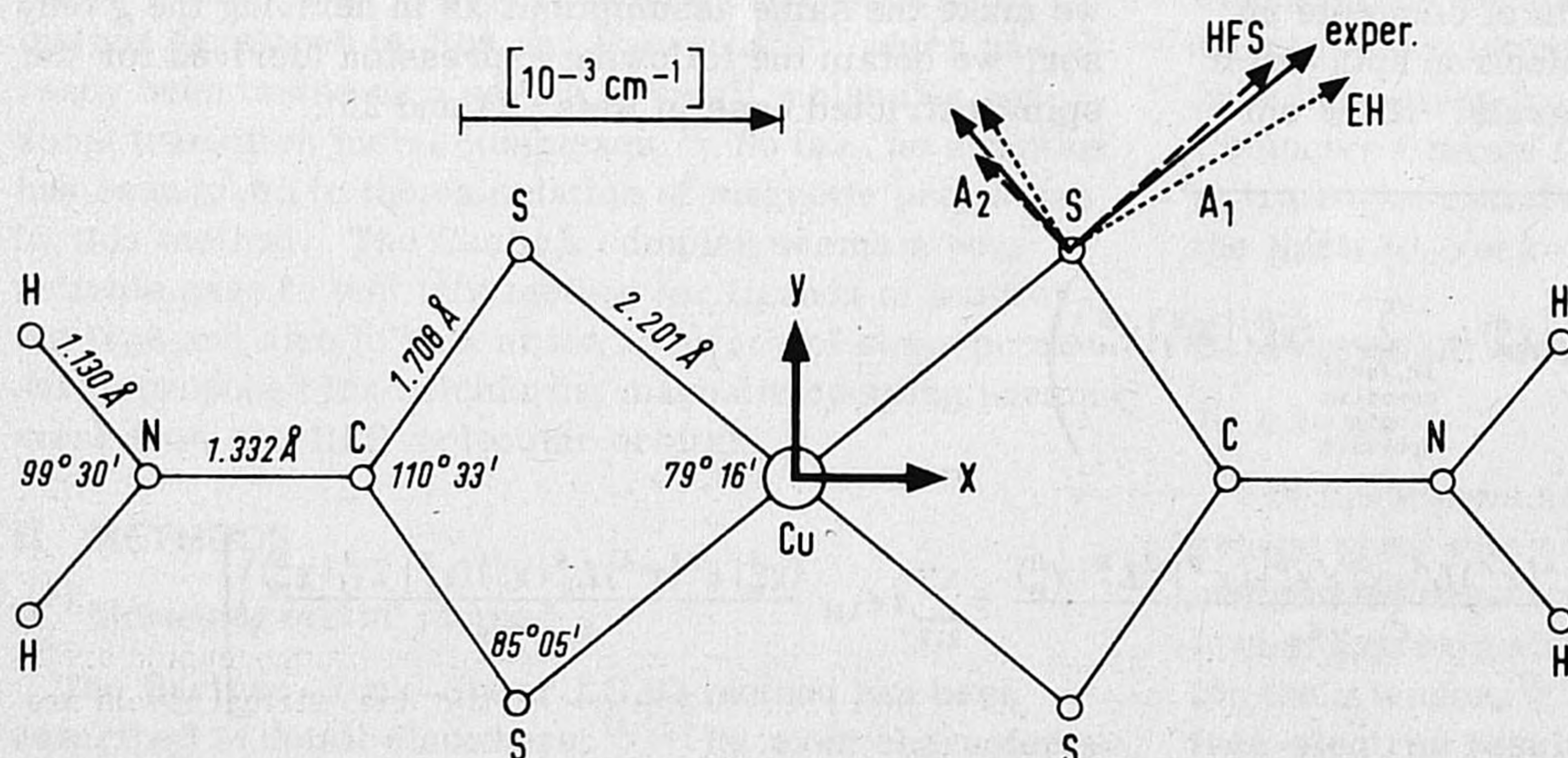


FIG. 1. Molecular structure (D_{2h}) of $\text{Cu}(\text{dte})_2$. Principal axes and values of hyperfine tensor on S (A_3 axis in the z direction).

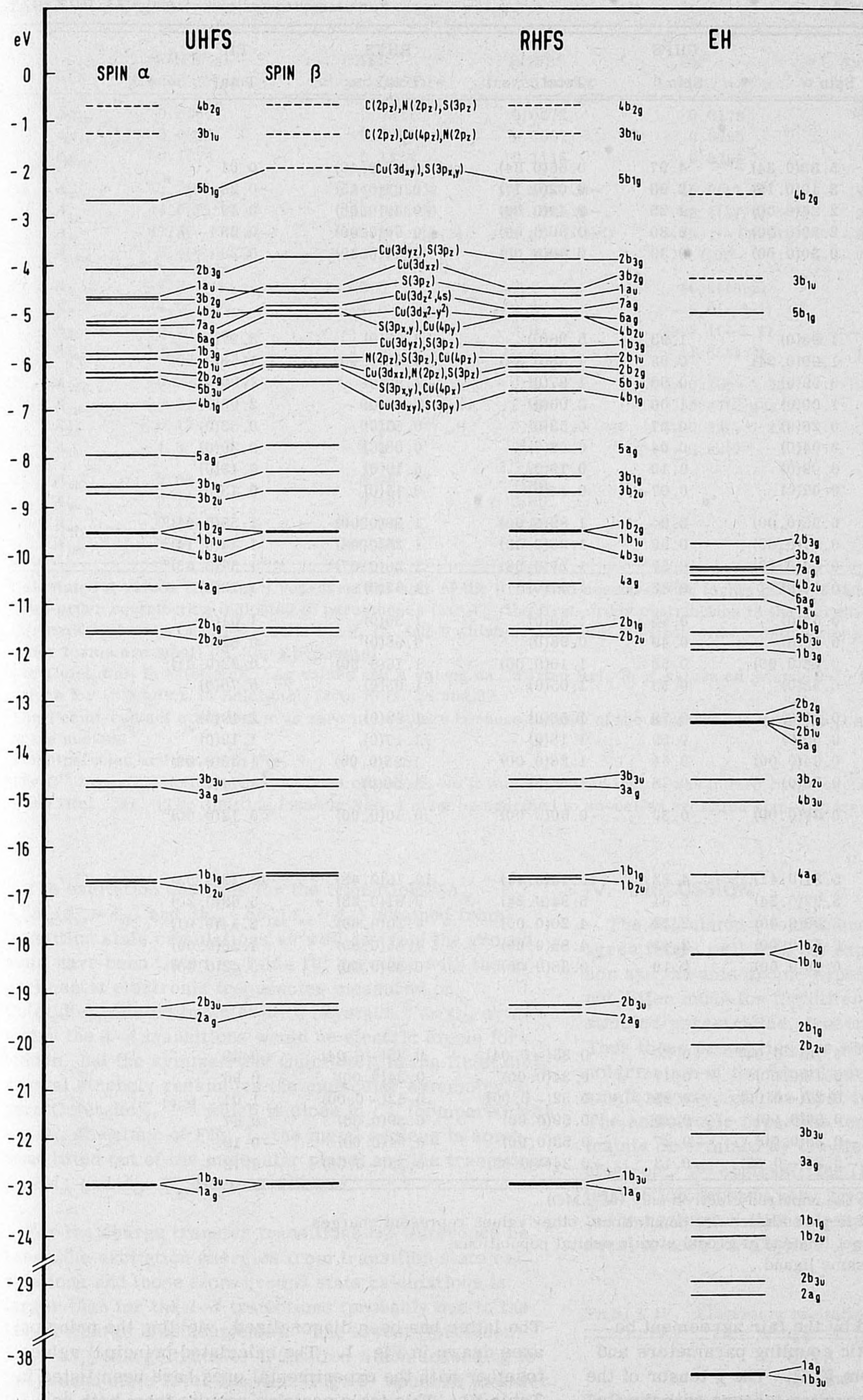


FIG. 2. Molecular orbital level scheme and main atomic orbital contributions to the highest occupied and lowest unoccupied orbitals for HFS (with frozen cores) and EH results in D_{2h} symmetry. Occupied levels are indicated by a solid line; virtual levels are indicated by a dashed line. The $5b_{1g}$ level holds one (unpaired) electron.

TABLE II. Population analysis.^a

	UHFS			RHFS		EH
	Spin α	Spin β	Total	Total	Total	
Gross atomic populations or charges ^b						
Cu	5.38(0.34)	4.97	0.66(0.34)	0.65(0.40)	0.01	
S	3.10(0.17)	2.93	-0.02(0.17)	-0.01(0.15)	-0.28	
C	2.24(0.00)	2.25	-0.49(0.00)	-0.49(0.00)	0.49	
N	2.80(0.00)	2.80	-0.60(0.00)	-0.60(0.00)	-0.50	
H	0.30(0.00)	0.30	0.40(0.00)	0.40(0.00)	0.28	
Gross atomic orbital populations						
Cu $3d_{z^2} + 3d_{x^2-y^2}$	1.93(0)	1.93	3.86(0)	3.85(0)	3.97(0)	
$3d_{xy}$	1.00(0.34)	0.58	1.58(0.34)	1.60(0.40)	1.58(0.53) ^c	
$3d_{xz}$	0.99(0)	0.98	1.97(0)	1.97(0)	1.99(0)	
$3d_{yz}$	1.00(0)	1.00	2.00(0)	2.00(0)	2.00(0)	
4s	0.26(0)	0.27	0.53(0)	0.53(0)	0.53(0)	
$4p_x$	0.04(0)	0.04	0.08(0)	0.08(0)	0.30(0)	
$4p_y$	0.09(0)	0.10	0.19(0)	0.19(0)	0.49(0)	
$4p_z$	0.07(0)	0.07	0.14(0)	0.14(0)	0.13(0)	
S 3s	0.95(0.00)	0.94	1.89(0.00)	1.89(0.00)	1.55(0.01) ^c	
$3p_x$	0.67(0.09)	0.59	1.26(0.09)	1.25(0.08)	1.44(0.14) ^c	
$3p_y$	0.64(0.08)	0.57	1.21(0.08)	1.20(0.07)	1.57(0.05) ^c	
$3p_z$	0.84(0)	0.83	1.67(0)	1.67(0)	1.73(0)	
C 2s	0.65(0)	0.65	1.30(0)	1.30(0)	1.01(0)	
$2p_x$	0.49(0)	0.49	0.98(0)	0.98(0)	0.82(0)	
$2p_y$	0.58(0.00)	0.58	1.16(0.00)	1.16(0.00)	0.92(0.01) ^c	
$2p_z$	0.52(0)	0.53	1.05(0)	1.05(0)	0.75(0)	
N 2s	0.79(0)	0.79	1.58(0)	1.58(0)	1.19(0)	
$2p_x$	0.59(0)	0.59	1.18(0)	1.17(0)	1.19(0)	
$2p_y$	0.64(0.00)	0.64	1.28(0.00)	1.28(0.00)	1.38(0.00) ^c	
$2p_z$	0.78(0)	0.78	1.56(0)	1.56(0)	1.74(0)	
H 1s	0.30(0.00)	0.30	0.60(0.00)	0.60(0.00)	0.72(0.00) ^c	
Net atomic populations						
Cu	5.31(0.41)	4.83	10.14(0.41)	10.16(0.48)	10.22(0.53)	
S	3.07(0.24)	2.84	5.91(0.24)	5.91(0.23)	5.69(0.20)	
C	2.08(0.00)	2.12	4.20(0.00)	4.20(0.00)	2.14(0.01)	
N	2.42(0.00)	2.43	4.85(0.00)	4.85(0.00)	4.38(0.00)	
H	0.19(0.00)	0.19	0.38(0.00)	0.39(0.00)	0.42(0.00)	
Atom-atom overlap populations						
Cu-S	0.16(-0.04)	0.20	0.36(-0.04)	0.35(-0.04)	0.45	
S-C	0.17(0.00)	0.17	0.34(0.00)	0.34(0.00)	0.96	
C-N	0.27(-0.00)	0.25	0.52(-0.00)	0.52(-0.00)	1.01	
N-H	0.30(0.00)	0.29	0.59(0.00)	0.59(0.00)	0.67	
Cu-C	-0.26(0.00)	-0.27	-0.53(0.00)	-0.54(0.00)	-0.12	
S-S ^d	-0.21(-0.09)	-0.13	-0.34(-0.09)	-0.33(-0.09)	-0.12	

^aValues in parentheses refer to the unpaired electron only ($5b_{1g}$ MO).

^bValues for spin α , spin β , and in parentheses are populations; other values represent charges.

^cEH values in parentheses are net (instead of gross) atomic orbital populations.

^dTwo S atoms belonging to the same ligand.

This picture is confirmed by the fair agreement between the calculated magnetic coupling parameters and the experimental values from EPR. The g tensor of the complex and the hyperfine coupling tensors with the Cu, S, C, and N nuclei have been calculated according to Eqs. (1), (3), and (4). Because of the D_{2h} symmetry of the complex and the positions of the nuclei, the principal axes of these tensors coincide with the molecular symmetry axes, except for the S hyperfine coupling tensor.

The latter has been diagonalized, yielding the principal axes drawn in Fig. 1. The calculated principal values, together with the experimental ones have been listed in Table III. This table contains results from both restricted and unrestricted HFS calculations with frozen cores and, since we expected spin polarization of the core electrons to be important especially for the Fermi-contact interaction with the Cu nucleus, we have also relaxed the Cu core orbitals in one calculation.

TABLE III. Magnetic coupling parameters.^a

	UHFS ^a frozen cores	UHFS ^a relaxed Cu core	RHFS ^a frozen cores	EH ^a	Experimental ^b	
	Δg_{xx}	0.0264	0.0271	0.0272	0.0179	0.0177(0.0207)
	Δg_{yy}	0.0330	0.0335	0.0367	0.0225	0.0227(0.0285)
	Δg_{zz}	0.1074	0.1124	0.1115	0.0755	0.0817(0.1053)
Cu	A_{xx}	43.2(56.5)	44.3(58.2)	38.5(52.3)	40.0(47.9)	43.0(43.8)
	A_{yy}	44.0(55.1)	45.0(56.8)	41.1(52.3)	39.1(47.9)	37.0(34.3)
	A_{zz}	-87.2(-111.5)	-89.3(-115.0)	-79.6(-104.7)	-79.1(-95.9)	-80.0(-78.2)
	A_{180}	5.4(-16.7)	-56.9(-80.0)	22.9(0) ^c	8.1(0) ^c	-79.0(-64.2)
S ^d	A_1	7.8	7.8	7.8	10.2(10.2)	9.9
	A_2	-4.0	-4.0	-3.9	-5.0(-5.1)	-5.5
	A_3	-3.8	-3.8	-3.9	-5.1(-5.1)	-4.4
	A_{180}	16.8	17.0	12.2	11.6(11.4)	11.7
C	A_{xx}	0.27	0.27	-0.00	-0.26(-0.22)	
	A_{yy}	-0.14	-0.14	0.01	0.47(0.44)	
	A_{zz}	-0.13	-0.13	-0.00	-0.22(-0.22)	< 2 ^e
	A_{180}	-4.8	-4.8	0 ^c	-0.02(0) ^c	
N	A_{xx}	0.08	0.08	-0.03		
	A_{yy}	0.16	0.16	0.05		
	A_{zz}	-0.24	-0.24	-0.03		
	A_{180}	-0.57	-0.56	0 ^c		

^aCalculated A values (10^{-4} cm^{-1}) represent the sum of the first- and second-order terms [Eqs. (3) and (4)], with the first-order contribution indicated in parentheses (for A_{180} the first-order contribution is the Fermi-contact term (3); exceptions are the HFS results for S, C, and N which contain only the first-order contributions, as the second-order terms are small (cf. the EH results).

^bFor $\text{Cu}(\text{et}_2\text{dte})_2$ in $\text{Ni}(\text{et}_2\text{dte})_2$, Δg values and A values on Cu from Ref. 3, A values on S from Ref. 4; in parentheses values for $\text{Cu}(\text{et}_2\text{dte})_2$ in $\text{Zn}(\text{et}_2\text{dte})_2$ from Refs. 24 and 30.

^cThe Fermi-contact contribution is zero in this case because the MO of the unpaired electron ($5b_{1g}$) has zero density at the nucleus.

^dPrincipal axes are shown in Fig. 1.

^eThe C^{13} hyperfine splitting has not been observed, so it was concluded that it was buried in the copper hyperfine line-width (Ref. 34). [The splitting found in Ref. 4 must be ascribed to so-called hydrogen spin-flip transitions (Ref. 35).]

The excitation energies for the transitions $2b_{3g} \rightarrow 5b_{1g}(d_{yz} \rightarrow d_{xy})$ and $3b_{2g} \rightarrow 5b_{1g}(d_{xz} \rightarrow d_{xy})$ obtained from transition state calculations as well as from the ground state have been listed in Table IV, together with the experimental electronic frequencies measured on $\text{Cu}(\text{et}_2\text{dte})_2$ diluted in $\text{Zn}(\text{et}_2\text{dte})_2$ crystals.⁶ In D_{2h} symmetry the $d-d$ transitions would be electric dipole forbidden, but the symmetry of $\text{Cu}(\text{et}_2\text{dte})_2$ in the $\text{Zn}(\text{et}_2\text{dte})_2$ crystal strongly resembles the molecular symmetry in pure $\text{Cu}(\text{et}_2\text{dte})_2$,^{30,31} which is close to C_{2v} (compared with the D_{2h} structure of Fig. 1, the metal nucleus is somewhat lifted out of the molecular plane) and the transitions $d_{yz} \rightarrow d_{xy}$ and $d_{xz} \rightarrow d_{xy}$ become allowed.

For the charge transfer transitions the difference between the excitation energies from transition state calculations and those from ground state calculations is larger than for the $d-d$ transitions (probably due to the larger charge displacements). The lowest (forbidden) $5b_{1g} \rightarrow 3b_{1u}$ charge transfer transition which according to the ground state level diagram (Fig. 2) would be at lower frequency than the lowest $d-d$ band, shifts to considerably higher energy in a transition state calculation. Its frequency becomes comparable with the $d-d$ transition frequencies; its intensity is probably very low as it is forbidden even in C_{2v} symmetry. The other charge transfer bands will be at higher frequencies.

IV. DISCUSSION

The calculated g tensor and hyperfine coupling tensors agree fairly well with the experimental data. The g tensor and the anisotropic hyperfine tensors on Cu and S do not differ much for the different HFS calculations (restricted/unrestricted, frozen core/relaxed Cu core). Thus these properties are not much affected by the spin polarization of the "doubly occupied" orbitals (which is small anyway, cf. the first two columns in Table II). The anisotropic hyperfine tensors, in particular, are mainly determined by the distribution of the unpaired electron. By contrast, the (isotropic) Fermi-contact interaction depends very strongly on spin polarization: in the restricted HFS calculation this term is exactly equal to zero for Cu (in D_{2h} symmetry; in the real mo-

TABLE IV. Electronic excitation energies (cm^{-1}).

Transition	UHFS (ground state)	UHFS (transition state)	Experimental ^a
$2b_{3g} \rightarrow 5b_{1g}(3d_{yz} \rightarrow 3d_{xy})$	14 820	15 990	14 480
$3b_{2g} \rightarrow 5b_{1g}(3d_{xz} \rightarrow 3d_{xy})$	19 840	21 670	18 600

^aFrom Ref. 6; our assignment of the experimentally observed bands is the reverse of that given by the authors (see text).

lecular C_i symmetry a very small positive value has been found from EH calculations⁸). The spin polarization of the valence orbitals makes this term negative (but still too small in absolute value), while the corresponding interaction on the S atoms remains positive (in agreement with the experimental results). The spin polarization of the Cu core increases the negative value for the isotropic Cu hyperfine coupling and it becomes in satisfactory agreement with experiment, considering the very small spin polarization responsible for this contact interaction. The remaining discrepancy could be due to the rather simple (single zeta) representation of the core orbitals and to the defect that the unrestricted HFS wave function is not an eigenfunction of the total spin operator. Also in the g tensor and anisotropic hyperfine tensors the remaining deviations from experiment are fairly small and could well be caused by the approximate formulas used for the calculation of these magnetic coupling parameters (e.g., the neglect of many-center integrals).

These deviations could also originate from the difference between the assumed $Ni(et_2dte)_2$ structure for the copper complex and the actual molecular $Cu(et_2dte)_2$ structure [e.g., the difference between the Cu-S bond length and the Ni-S bond length is about 0.1 Å (Ref. 32)] or from the interactions with neighbors in the crystal. In this respect, it is very interesting to compare the EPR parameters measured on $Cu(et_2dte)_2$ in $Zn(et_2dte)_2$ (see Table III), which happen to agree even better with the HFS calculations than the nickel crystal parameters.

Because of the fair overall agreement, we conclude that the MO picture emerging from the HFS-LCAO calculations, the charge distribution, the degree of covalency, and the delocalization of the unpaired electron are realistic. This picture agrees with the EH results,^{8,9} calculated with two of the parameters fitted to the experimental g tensor, and it confirms some more empirical interpretations of the EPR results.³³

The excitation energies from our HFS calculations agree quite well with the experimental optical spectrum; the assignment of the $d-d$ transitions also agrees with EH.⁸ So the assignment by Rajasekharan *et al.*⁶ is probably incorrect. (This assignment could not be based on the polarization of the measured electronicspectrum since the molecules in the crystal are not oriented along the polarization directions. Instead, the authors⁶ have invoked an approximate electrostatic model.) Surprisingly, the excitation energies from the ground state HFS calculation are even better than those from transition state calculations. We may ascribe this to neighbor effects or geometry distortions in the $Cu(et_2dte)_2$ molecules, built into $Zn(et_2dte)_2$ crystals (the actual molecular symmetry being close to C_{2v} , while the HFS calculations have been performed on D_{2h} symmetry molecules). All HFS results are considerably better than the EH excitation energies, which are unrealistically high (38650 and 42420 cm^{-1} for the $d-d$ transitions).

Concluding we may say that our results for $Cu(dte)_2$ illustrate that the nonempirical HFS-LCAO method can be well used to calculate not only the charge distribution in transition metal complexes, but also various magnetic and optical properties.

ACKNOWLEDGMENTS

We thank Professor Dr. P. Ros, Dr. E. J. Baerends, and Dr. W. Heijser for making available and for assistance in using the HFS-LCAO program. We are grateful to Dr. C. P. Keijzers for stimulating discussions and for making available his programs to calculate the magnetic coupling tensors in the restricted Hartree-Fock case. The investigations were supported (in part) by the Netherlands Foundation for Chemical Research (SON) with financial aid from the Netherlands Organization for the Advancement of Pure Research (ZWO).

- ¹J. Willemse, J. A. Cras, J. J. Steggerda, and C. P. Keijzers, *Struct. Bonding* (Berlin) **28**, 83 (1976).
- ²D. Coucouvanis, *Prog. Inorg. Chem.* (in press).
- ³M. J. Weeks and J. P. Fackler, *Inorg. Chem.* **7**, 2548 (1968).
- ⁴R. Kirmse and B. V. Solovev, *J. Inorg. Nucl. Chem.* **39**, 41 (1977).
- ⁵Hyunsoo So and R. Linn Belford, *J. Am. Chem. Soc.* **91**, 2392 (1969).
- ⁶M. V. Rajasekharan, C. N. Sethulakshmi, P. T. Manoharan, and H. Gudel, *Inorg. Chem.* **15**, 2657 (1976).
- ⁷J. G. M. van der Linden, thesis, Nijmegen, 1972.
- ⁸C. P. Keijzers, H. J. M. de Vries, and A. van der Avoird, *Inorg. Chem.* **11**, 1338 (1972).
- ⁹C. P. Keijzers and E. de Boer, *Mol. Phys.* **29**, 1007 (1975).
- ¹⁰E. J. Baerends, D. E. Ellis, and P. Ros, *Chem. Phys.* **2**, 41 (1973).
- ¹¹E. J. Baerends and P. Ros, *Chem. Phys.* **2**, 52 (1973).
- ¹²E. J. Baerends and P. Ros, *Int. J. Quantum Chem. Symp.* **12**, 169 (1978).
- ¹³J. C. Slater, *Quantum Theory of Molecules and Solids* (McGraw-Hill, New York, 1974), Vol. 4.
- ¹⁴K. H. Johnson, *J. Chem. Phys.* **45**, 3085 (1966).
- ¹⁵H. Sambe and R. H. Felton, *J. Chem. Phys.* **62**, 1122 (1975).
- ¹⁶E. Clementi and C. Roetti, *Atomic Data and Nuclear Data Tables* (Academic, New York, 1974), Vol. 14, p. 177ff.
- ¹⁷E. J. Baerends and P. Ros, *Mol. Phys.* **30**, 1735 (1975).
- ¹⁸A. J. Stone, *Proc. R. Soc. London A* **271**, 424 (1963).
- ¹⁹C. P. Slichter, *Principles of Magnetic Resonance* (Harper and Row, New York, 1963).
- ²⁰J. C. Slater, *Quantum Theory of Atomic Structure* (McGraw-Hill, New York, 1960), Vol. 2, p. 189ff.
- ²¹W. H. Moores and R. McWeeny, *Proc. R. Soc. London A* **332**, 365 (1973).
- ²²P. W. Langhoff, M. Karplus, and R. P. Hurst, *J. Chem. Phys.* **44**, 505 (1966).
- ²³E. Ishiguro and M. Kobori, *J. Phys. Soc. Jpn* **22**, 263 (1967).
- ²⁴C. P. Keijzers, thesis, Nijmegen, 1974.
- ²⁵C. P. Keijzers and E. de Boer, *J. Chem. Phys.* **57**, 1277 (1972).
- ²⁶A. Lichnerowicz, *Elements of Tensor Calculus* (Methuen, London, 1962).
- ²⁷T. Amos and L. C. Snyder, *J. Chem. Phys.* **41**, 1773 (1964).
- ²⁸M. Bonamico, G. Dessy, C. Mariani, A. Vaciago, and L. Zambonelli, *Acta Crystallogr.* **19**, 619 (1965).
- ²⁹C. P. Keijzers, G. F. M. Paulussen, and E. de Boer, *Mol. Phys.* **29**, 973 (1975).
- ³⁰C. P. Keijzers, P. L. A. C. M. van der Meer, and E. de Boer, *Mol. Phys.* **29**, 1733 (1975).
- ³¹C. P. Keijzers and E. de Boer, *Mol. Phys.* **29**, 1743 (1975).
- ³²M. Bonamico, G. Dessy, A. Mugnoli, A. Vaciago, and L. Zambonelli, *Acta Crystallogr.* **19**, 886 (1965).
- ³³T. R. Reddy and R. Srinivasan, *J. Chem. Phys.* **43**, 1404 (1965).
- ³⁴H. J. Stoklosa and J. R. Wasson, *Inorg. Nucl. Chem. Lett.* **10**, 377 (1974).
- ³⁵D. Attanasio, *Inorg. Chem.* **16**, 1824 (1977).